

Ni(OH)₂ Derived from NiS₂ Induced by Reflux Playing Three Roles for Hydrogen/Oxygen Evolution Reaction

Sheng-Jun Xu^{1*}, Ya-Nan Zhou², Guo-Ping Shen² and Bin Dong^{2*}

¹Dongying Haikou Ruilin Chemical Co., LTD., Dongying 257000, China

²State Key Laboratory of Heavy Oil Processing, College of Chemistry and Chemical Engineering, China University of Petroleum (East China), Qingdao 266580, China

*Corresponding authors. Emails: 18905469551@163.com (S.J. Xu) and dongbin@upc.edu.cn (B. Dong)

n CHARACTERIZATION

The crystal phase of the obtained catalysts was studied via X-ray diffraction (XRD) on a Rigaku D/max-2500pc device with Cu K α radiation ($\lambda = 1.54 \text{ \AA}$). The Raman spectra were gained by LabRAM HR evolution with an excitation wavelength of 514 nm. The scanning electron microscope (SEM) (Hitachi S-4800) and Transmission Electron Microscope (TEM) (FEI Tecnai G20, 200 kV) were applied to collect the information of morphological and structural information of all samples. The element composition and distribution on catalysts were detected by means of the Energy Dispersive System (EDS) and detected on the Hitachi S-4800. The X-ray photoelectron spectroscopy (XPS) is characterized by a Thermo Fisher Scientific II spectrometer. Electron paramagnetic resonance (EPR) was used to obtain the information about oxygen vacancies concentration.

n ELECTROCHEMICAL MEASUREMENTS

The OER performance of all the catalysts was evaluated in a standard three-electrode cell configuration on Gamry Reference 600 electrochemical equipment in 1.0 M KOH at room temperature. This process was performed with the Pt foil (OER)/carbon electrode (HER), saturated calomel electrode and catalyst samples deposited on glassy carbon as the counter electrode, reference electrode, and working electrode, respectively. The 5 mg catalyst powder was dissolved in a 1 mL dilute solution of a mixture of Nafion, ethanol and water. Then 5 μL of the solution was dropped onto a glassy carbon electrode with a diameter of 3 mm. The linear sweep voltammetry (LSV) was gained at the same condition with a scan rate of 2 mV s^{-1} . All the potentials vs. SCE were converted into a standard reversible hydrogen electrode (RHE) by means of the Nernst equation: $E_{\text{RHE}} = E_{\text{SCE}} + 0.0594 \text{ pH} + 0.242$. The cyclic voltammetry (CV) curves were tested at 40, 60, 80, 100, 120 mV s^{-1} and were used to determine the electrical double-layer capacitances (C_{dl}). And electrochemical impedance spectroscopy (EIS) was performed at 1.56 V vs. SCE (OER)/0.35 V vs. SCE (HER) and the frequency ranges from 10^5 to 0.1 Hz. The stability of the final sample was performed by CV curves for 2000 cycles at 40 mV s^{-1} and chronoamperometry.

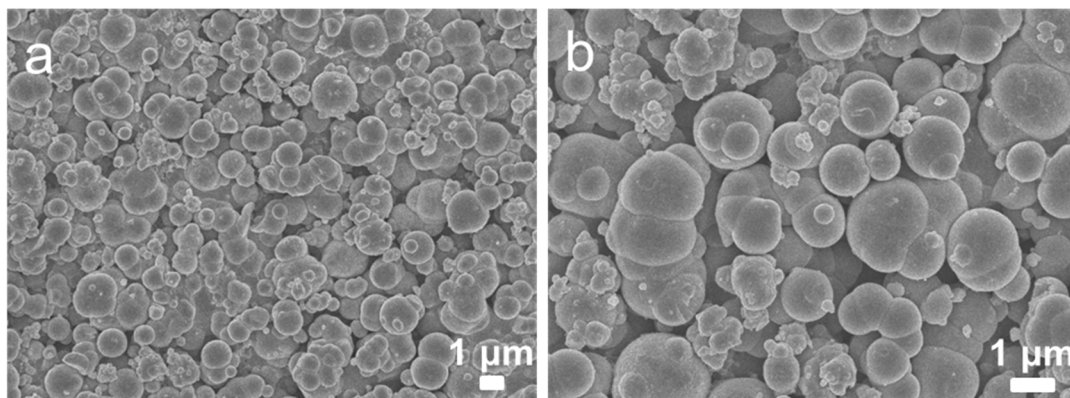


Figure S1. SEM images of NiS₂ with the hydrothermal time shorter than 2 h.

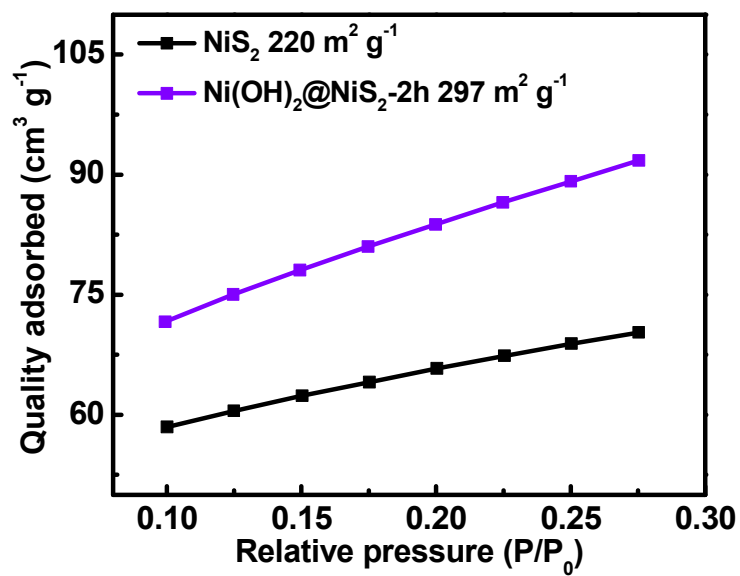


Figure S2. BET characterization of NiS₂ and Ni(OH)₂@NiS₂-2h.

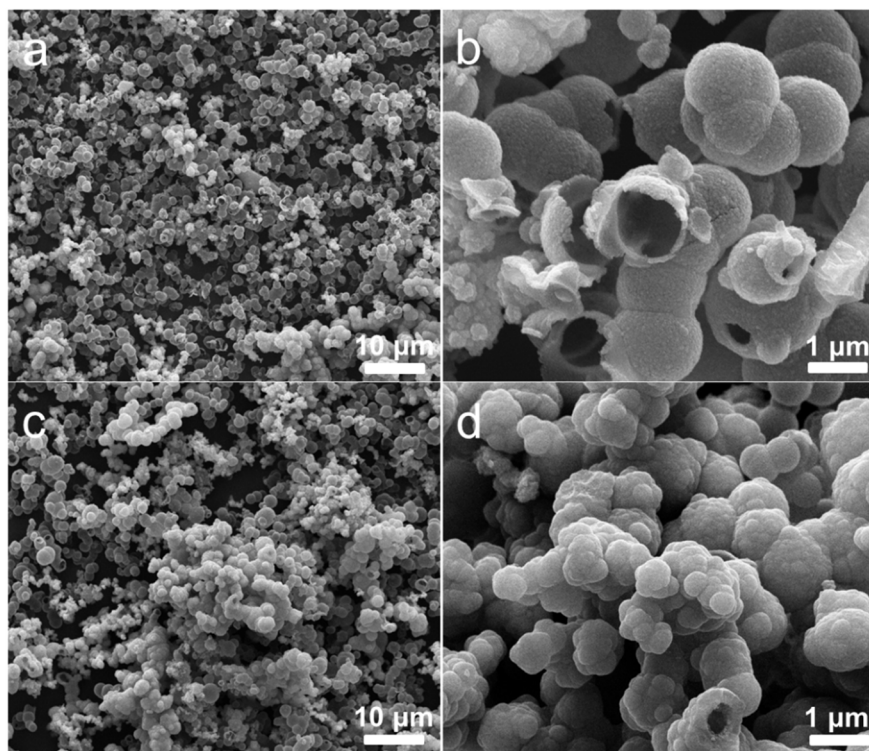


Figure S3. SEM images of (a,b) $\text{Ni(OH)}_2\text{@NiS}_2\text{-1h}$ and (c,d) $\text{Ni(OH)}_2\text{@NiS}_2\text{-3h}$.

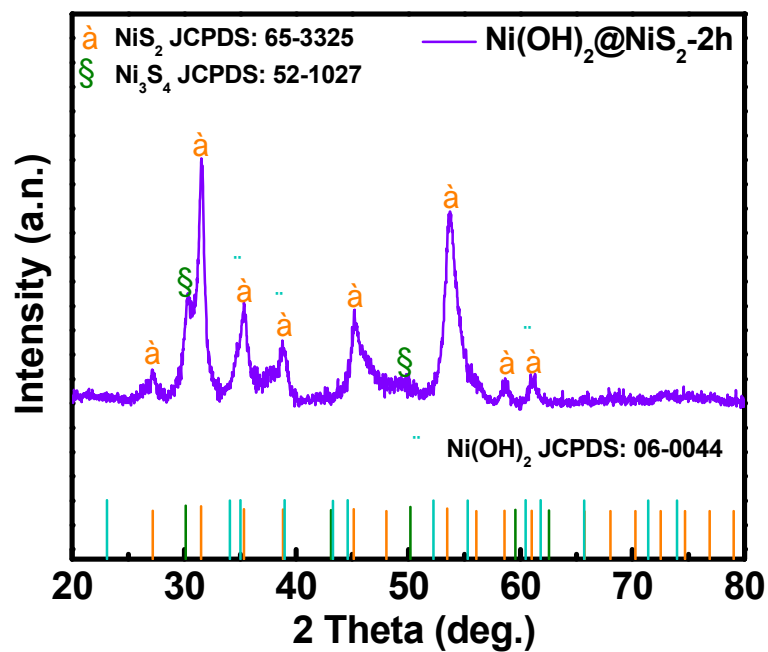


Figure S4. XRD of $\text{Ni(OH)}_2@\text{NiS}_2\text{-2h}$, where the Ni(OH)_2 and NiS_x peaks can be observed.

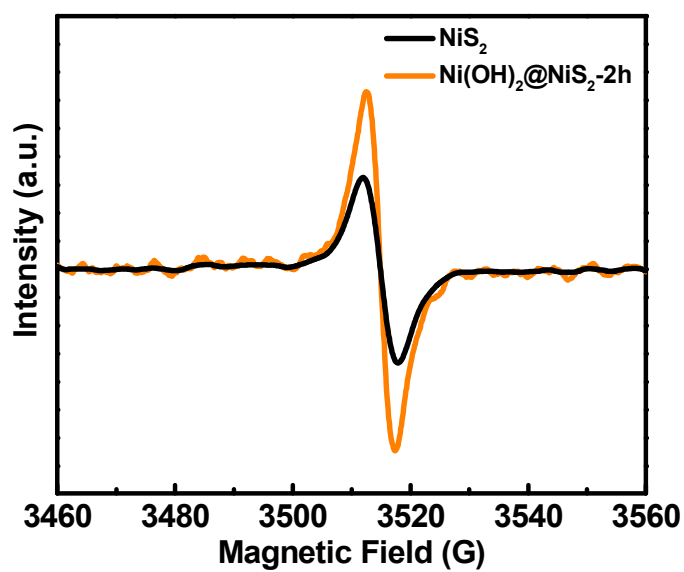


Figure S5. EPR of NiS_2 and $\text{Ni(OH)}_2@\text{NiS}_2\text{-2h}$ ($g = 2.000$).

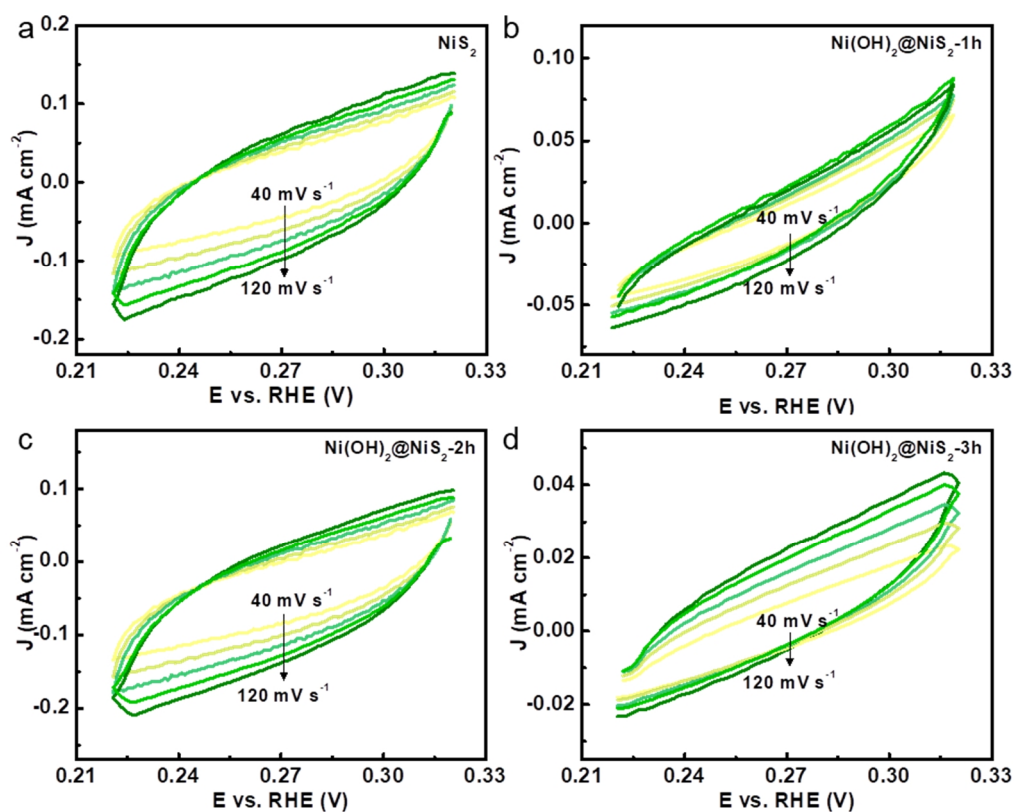


Figure S6. CV curves of (a) NiS_2 , (b) $\text{Ni(OH)}_2@\text{NiS}_2\text{-1h}$, (c) $\text{Ni(OH)}_2@\text{NiS}_2\text{-2h}$ and (d) $\text{Ni(OH)}_2@\text{NiS}_2\text{-3h}$ with the scan rate of 40, 60, 80, 100 and 120 mV s^{-1} .

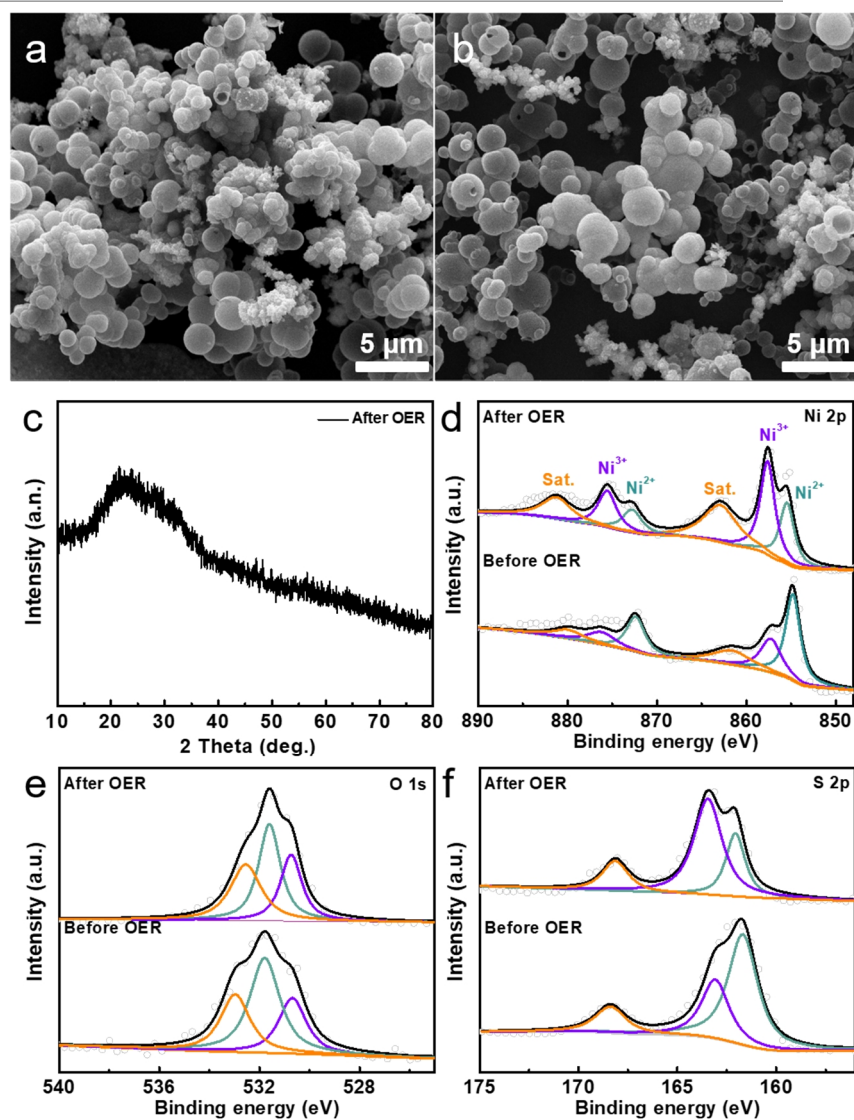


Figure S7. SEM images of $\text{Ni(OH)}_2@\text{NiS}_2\text{-2h}$ after (a) OER and (b) HER. (c) XRD, (d) Ni 2p, (e) O 1s and (f) S 2p of $\text{Ni(OH)}_2@\text{NiS}_2\text{-2h}$ after OER.

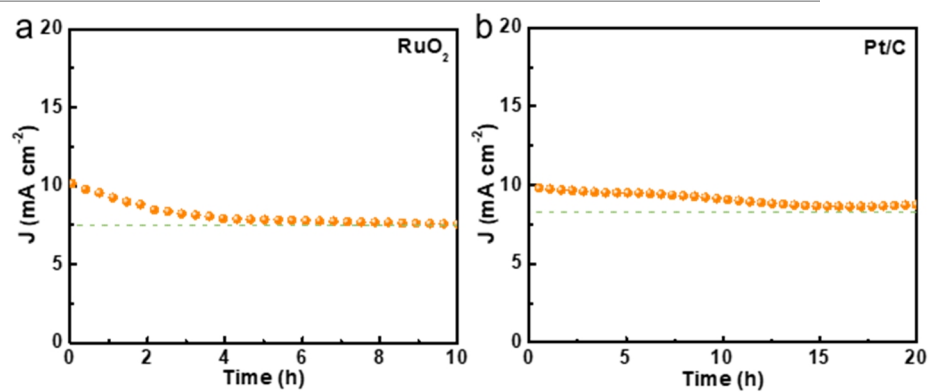


Figure S8. I - t curves of (a) RuO_2 and (b) Pt/C .

Table S1. Comparison of OER Performance in Alkaline Media for NiS with the Previous Catalysts.

Catalysts	η_{10} (mV)	Tafel slope (mV dec ⁻¹)	Reference
Ni(OH) ₂ @NiS-2h	309	51.7	This work
NiS	320	59	1
NiS/Ni	330	67	2
NiS@N/S-C	417	48	3
NiS-based	337	53.2	4
NiS	354	116	5
P-CoS	340	73	6
CoS-Oct	325	77	7
NiCu-LDH@CoS/g-C ₃ N ₄	290	75	8
ED-CoS	310	55	9
Co ₃ O ₄ /CoS	349	66.6	10
CoS (1:0.5)	383	38	11
FeS	320	69	12

Table S2. Comparison of HER performance in alkaline media for NiS with the previous catalysts.

Catalysts	η_{10} (mV)	Tafel slope (mV dec ⁻¹)	Reference
Ni(OH) ₂ @NiS-2h	233	151.5	This work
P30-doped Fe/NF	158.17	105.2	13
CoS-Oct	200	126	14
CoSP/NC	183	64.25	15
CoFeS/NC	176	67.8	16
CoS-30 in neutral water	233	71	17
NiCo ₂ S ₄	345	60	18
Ag ₂ S-CoS	275	77.1	19
NiS/Ni(OH) ₂	196	133	20
NiS/FTO	290	143.4	21
NiS/Ni	161	74	22
Ni ₃ S ₂ /NiS/NOSC-900	180	83	23

n REFERENCES

- (1) Luo, P.; Zhang, H. J.; Liu, L.; Zhang, Y.; Deng, J.; Xu, C. H.; Hu, N.; Wang, Y. Targeted synthesis of unique nickel sulfide (NiS, NiS microarchitectures and the applications for the enhanced water splitting system. *ACS Appl. Mater. Interfaces* **2017**, 9, 2500-2508.
- (2) Adeel, M.; Gul, R.; Anwar, H. A. S.; Oh-shim, J.; Shabeer, A. M. Template-free hydrothermal growth of nickel sulfide nanorods as high-performance electroactive materials for oxygen evolution reaction and supercapacitors. *Energy Fuels* **2021**, 35, 6868-6879.
- (3) Yang, L.; Gao, M.; Dai, B.; Guo, X.; Liu, Z.; Peng, B. An efficient NiS@N/S-C hybrid oxygen evolution electrocatalyst derived from metal-organic framework. *Electrochim. Acta* **2016**, 191, 813-820.
- (4) Wang, L.; Cao, L. L.; Liu, X. K.; Zhang, W.; Liu, W.; Shen, X. Y.; Wang, Y.; Yao, T. Strong Ni-S hybridization in crystalline NiS electrocatalyst for robust acidic oxygen evolution. *J. Phys. Chem. C* **2020**, 124, 5, 2756-2761.
- (5) Dai, W. J.; Pan, Y.; Wang, N.; Wu, S. K.; Li, X. Z.; Zhu, Y. A.; Lu, T. Nanocrystalline NiS particles synthesized by mechanical alloying as a promising oxygen evolution electrocatalyst. *Mater. Lett.* **2018**, 218, 115-118.
- (6) Jiang, J. H.; Xu, J. L.; Wang, W. W.; Zhang, L.; Xu, G. C. Phosphate ion-functionalized CoS with hexagonal bipyramid structures from metal-organic framework: bifunctionality towards supercapacitors and oxygen evolution reaction. *Chem. Eur. J.* **2020**, 26, 14903-14911.
- (7) Akram, R.; Khan, M. D.; Zequine, C.; Zhao, C.; Gupta, R. K.; Akhtar, M.; Akhtar, J.; Malik, M. A.; Revaprasadu, N.; Bhatti, M. H. Cobalt sulfide nanoparticles: synthesis, water splitting and supercapacitance studies. *Mater. Sci. Semicond. Proc.* **2020**, 109, 104925.
- (8) Kotes, K. M.; Namgyu, S.; Misook, K. Enhanced electrocatalytic activity by NiCu-LDH/CoS as dual co-catalysts on g-C₃N₄ nanosheets in NiCu-LDH@CoS/g-C₃N₄ nanostructure for oxygen evolution reactions. *Appl. Surf. Sci.* **2022**, 593 153453.
- (9) Nan, K. K.; Du, H. F.; Su, L.; Li, C. M. Directly electrodeposited cobalt sulfide nanosheets as advanced catalyst for oxygen evolution reaction. *ChemistrySelect* **2018**, 3, 7081-7088.
- (10) Min, K.; Kim, S. J.; Lee, E.; Yoo, G.; Ham, H. C.; Sang Shim, E.; Lim, D.; Baek, S.-H. A hierarchical Co₃O₄/CoS microbox heterostructure as a highly efficient bifunctional electrocatalyst for rechargeable Zn-air batteries. *J. Mater. Chem. A* **2021**, 9, 17344-17352.
- (11) Adamson, W.; Jia, C.; Li, Y. B.; Zhao, C. Cobalt oxide micro flowers derived from hydrothermal synthesised cobalt sulphide pre-catalyst for enhanced water oxidation. *Electrochim. Acta* **2020**, 355, 136802.
- (12) Ayyavu, S.; Rajasekaran, E.; Govindhan, M. Self-supported fabrication and electrochemical water splitting study of transition-metal sulphides nanostructured electrodes. *New J. Chem.* **2020**, 44, 5071-5078.
- (13) Ju, Y.; Feng, S. Y.; Wang, X. B.; Li, M.; Wang, L.; Xu, R. D.; Wang, J. L. Facile preparation of a porous nanosheet P-doped Fe Bi-functional catalyst with excellent OER and HER electrocatalytic activity. *ChemistrySelect* **2021**, 6, 4979-4990.
- (14) Akram, R.; Khan, M. D.; Zequine, C.; Zhao, C.; Gupta, R. K.; Akhtar, M.; Akhtar, J.; Malik, M. A.; Revaprasadu, N.; Bhatti, M. H. Cobalt sulfide nanoparticles: synthesis, water splitting and supercapacitance studies. *Mater. Sci. Semicond. Proc.* **2020**, 109, 104925.
- (15) Zhao, L. P.; Yang, A. L.; Wang, A. Q.; Yu, H.; Dai, J.; Zheng, Y. J. Metallic Co, CoS, and P co-doped N enriched carbon derived from ZIF-67 as an efficient catalyst for hydrogen evolution reaction. *Int. J. Hydrogen Energy* **2020**, 45, 30367-30374.
- (16) Wu, S. C.; Yang, X. R. ZIF-67-derived N-enriched porous carbon doped with Co, Fe and CoS for electrocatalytic hydrogen evolution reaction. *Environ. Res.* **2021**, 200, 111474.
- (17) You, B.; Jiang, N.; Sun, Y. J. Morphology-activity correlation in hydrogen evolution catalyzed by cobalt sulfides. *Inorg. Chem. Front.* **2016**, 3, 279-285.
- (18) Aftab, U.; Tahira, A.; Mazzaro, R.; Morandi, V.; Ishaq Abro, M.; Baloch, M. M.; Yu, Cong; Ibupoto, Z. H. Nickel cobalt bimetallic sulfide NiCo₂S₄ nanostructures for a robust hydrogen evolution reaction in acidic media. *RSC Advances* **2020**, 10, 22196-22203.
- (19) Lee, C.; Lee, C.; Shin, K.; Song, T.; Jeong, H. Y.; Jeon, D. Y.; Lee, H. M. Ag₂S-CoS hetero-nanowires terminated with stepped surfaces for improved oxygen evolution reaction. *Catal. Commun.* **2019**, 129, 105749.
- (20) Kandiel, T. A. Iron-incorporated NiS/Ni(OH)₂ composite as an efficient electrocatalyst for hydrogen evolution reaction from water in a neutral medium. *Appl. Catal. A Gen.* **2019**, 586, 117226.
- (21) Rahman, G.; Chae, S. Y.; Joo, O. S. Efficient hydrogen evolution performance of phase-pure NiS electrocatalysts grown on fluorine-doped tin oxide-coated glass by facile chemical bath deposition. *Int. J. Hydrogen Energy* **2018**, 43, 13022-13031.
- (22) Yan, C. Y.; Huang, J. W.; Wu, C. Y.; Li, Y. Y.; Tan, Y. C.; Zhang, L. Y.; Sun, Y. H.; Huang, X. N.; Xiong, J. In-situ formed NiS/Ni coupled interface for efficient oxygen evolution and hydrogen evolution. *J. Mater. Sci. Technol.* **2020**, 42, 10-16.
- (23) Cao, Y. F.; Meng, Y. Y.; Huang, S. C.; He, S. M.; Li, X. H.; Tong, S. F.; Wu, M. M. N-, O- and S-doped carbon-encapsulated Ni₃S₂ and NiS Core-Shell architectures: bifunctional electrocatalysts for hydrogen evolution and oxygen reduction reactions. *ACS Sustainable Chem. Eng.* **2018**, 6, 15582-15590.